UNCLASSIFIED

AD NUMBER

AD871326

NEW LIMITATION CHANGE

TO

Approved for public release, distribution unlimited

FROM

Distribution authorized to U.S. Gov't. agencies and their contractors; Critical Technology; JUN 1970. Other requests shall be referred to Air Force Materials Laboratory, ATTN: MAAM, Wright-Patterson AFB, OH 45433.

AUTHORITY

AFML ltr dtd 12 Jan 1972

THIS PAGE IS UNCLASSIFIED

(20)

MAY-JUNE, 1970 NO. 22

CERAMIC AWARENESS BULLETIN

- NEW R & D
- DIGESTS OF SELECTED ACCESSIONS

SPECIAL NOTE: DIBORIDES FOR LIFTING RE-ENTRY VEHICLE COMPONENTS

DCIC
DEFENSE CERAMIC INFORMATION CENTER

A Department of Defense information
analysis center

A focal point in acquiring, evaluating,
and disseminating authoritative, timely
information about ceramic materials of
interest to the Department of Defense,
other Government agencies, their con-
tractors, and their suppliers

This document is subject to special export controls and each transmittal to foreign governments or foreign nationals may be made only with prior approval of the Air Force Materials Laboratory.
attn: MAAM, W-P-AFB, Ohio 45433

21

DCIC
DEFENSE CERAMIC INFORMATION CENTER

MISSION

The Center collects, interprets, and disseminates technical information about ceramics for Department of Defense needs.

SCOPE

The Center's coverage and acquisitions, selected primarily on the basis of material composition, includes borides, carbides, carbon (graphite), nitrides, oxides, sulfides, silicides, and selected intermetallic compounds and glasses in the form of monophase and polyphase ceramic bodies, coatings, fibers, composites, and foams.

The subject fields include applications, property and performance data, processing and fabricating methods, testing methods, and fundamental aspects of processing and behavior of these materials.

SPONSOR

Air Force Materials Laboratory
Materials Support Division (MAAM)
Wright Patterson Air Force Base, Ohio

SERVICES

The services of the Center include answering technical inquiries, providing technical advisory services, and publishing data compilations, critical technical reviews, and news of recent developments.

QUALIFIED USERS

U. S. Government agencies, their contractors, suppliers, and others in a position to assist the defense effort.

ADDRESS

Defense Ceramic Information Center
Battelle Memorial Institute
Columbus Laboratories
505 King Avenue
Columbus, Ohio 43201
Telephone: Area Code 614, 299-3151
Extension 2758

NOTICES

This document is subject to special export controls and each transmittal to foreign governments or foreign nationals may be made only with prior approval of the Air Force Materials Laboratory.

Qualified requestors may obtain subsequent issues of the "Ceramic Awareness Bulletin" by writing or calling the Defense Ceramic Information Center at the address given above.

NEW R and D

APPLICATIONS

Development of Flightworthy Advanced Composite Structural Hardware for Missile and Spacecraft Applications

Goodyear Aerospace Corporation
Akron, Ohio 44315
Contract F33615-70-C-1390
Air Force Materials Laboratory/R. L. Rapson (MAC)

Evaluation of Laminated Porous Material for High-Temperature Air-Cooled Turbine Blades

General Motors Corporation
Allison Division
Indianapolis, Indiana 46206
Contract NAS3-13431
NASA, Lewis Research Center

Evaluation of Cryogenic Filament-Wound Tank

Aerojet-General Corporation
Azusa, California 91702
Contract NAS3-13326
NASA, Lewis Research Center

Lithium Hydride Shields

North American Rockwell Corporation
Atomics International
Canoga Park, California 91304
Contract NAS3-13466
NASA, Lewis Research Center

Development of Improved Cadmium Sulfide Solar Cells

Clevite Corporation
Subsidiary of Gould, Inc.
Cleveland, Ohio 44108
Contract NAS3-13467 (continuation of NAS3-11845)
NASA, Lewis Research Center/L. Scudder

Evaluation of Insulation Materials and Composites for Use in a Nuclear Radiation Environment

General Dynamics Corporation
Fort Worth Division
Fort Worth, Texas 76101
Contract NAS8-25848
NASA, Marshall Space Flight Center

Research on Cadmium Telluride Infrared Electro-Optical Modulator Crystals

Hughes Research Laboratories
Malibu, California 90265
Contract N00014-70-C-0303
Office of Naval Research

Development of Composite Materials With Improved Rain Erosion Resistance

Hughes Aircraft Company
Research and Development Division
Culver City, California 90232
Contract N00019-70-C-0315
Naval Air Systems Command/M. Stander (AIR-52033D)

Investigate the Choice Sensor Materials With Appropriate Stress Properties and Design Configuration Required for Development of a Gas Laser Accelerometer

North American Rockwell Corporation
Autonetics Division
Anaheim, California 92803
Contract N00019-70-C-0317
Naval Air Systems Command

Research and Development Program Directed Toward Obtaining a High-Temperature, Rain-Erosion-Resistant Coating System Suitable for Spray Application to Radomes and Other Leading-Edge Resin-Bonded Fiberglass Composite Structures of Supersonic Naval Aircraft

Southern Research Institute
Birmingham, Alabama 35205
Contract N00019-70-C-0330
Naval Air Systems Command/A. M. Malloy (AIR-52033)

Investigation of Crystal-Bearing Glass Filaments as Sensors for NDT

General Electric Company
Valley Forge Space Technology Center
Philadelphia, Pennsylvania 19101
Contract N00019-70-C-416
Naval Air Systems Command/M. Stander (AIR-52032D)

NEW R and D

Research and Development in the Field of Nonlinear High-Power Dielectrics

State of the Art, Inc.
State College, Pennsylvania 16801
Contract DAAB07-70-C-0191
Army Electronics Command/H. Stout (AMSEL KL-EC)

PROCESSING

Development of Fabrication Techniques for Boron/Aluminum Aircraft Structures

General Dynamics Corporation
Convair Division
San Diego, California 92112
Contract F33615-70-C-1460
Air Force Materials Laboratory/Andrew W. Davis (MAC)

Study of Convection in Crystal Growth for Spacing Processing

Lockheed Aircraft Corporation
Lockheed Missile and Space Company
Research and Engineering Center
Huntsville, Alabama 35907
Contract NAS8-25577
NASA, Marshall Space Flight Center/T. Bannister

Research Study on Composite Castings

Arthur D. Little, Inc.
Cambridge, Massachusetts 02140
Contract NAS8-25709 (continuation of NAS8-21402)
NASA, Marshall Space Flight Center/E. A. Hasemeyer

Ceramic Systems for Use as Structural Components in Hypersonic Missile Applications

Georgia Tech Research Institute
Atlanta, Georgia 30332
Contract N00017-70-C-4438 (continuation of N00017-67-C-0053)
Naval Ordnance Systems Command

Exploratory Development Program to Provide Improved Strength High Reliability Composite Material

Commonwealth Scientific Corporation
Alexandria, Virginia 22314
Contract N00017-70-C-4439
Naval Ordnance Systems Command

Investigation on the Preparation and Properties of Polycrystalline Refractory Oxides

AVCO Corporation
Applied Technology Division
Lowell, Massachusetts 01851
Contract N00019-70-C-0171 (continuation of N00019-69-C-0198)
Naval Air Systems Command

Investigate the Effects of Surface Finishing Treatments on the Properties of Structural Ceramics

Stanford Research Institute
Menlo Park, California 94025
Contract N00019-70-C-0179 (continuation of N00019-69-C-0229)
Naval Air Systems Command

Epitaxial Growth Techniques of Mercury Cadmium Telluride

International Business Machine Corporation
Electronic Systems Center
Owego, New York 13827
Contract N00019-70-C-0289
Naval Air Systems Command

Chemical Strengthening of Polycrystalline Ceramics

Ceramic Finishing Company
State College, Pennsylvania 16801
Contract N00019-70-C-0418 (continuation of N00019-69-C-0225)
Naval Air Systems Command

Investigation of Significant Variables Leading to the Development of Surface Treatments for High-Modulus Graphite Filaments

Philco-Ford Corporation
Aeronutronic Division
Newport Beach, California 92663
Contract N00019-70-C-0439 (continuation of N00019-69-C-0135)
Naval Air Systems Command

High-Capacitance Thin-Film Structures

General Telephone & Electronics Laboratories, Inc.
Bayside, New York 11360
Contract DAAB07-70-C-0169
Army Electronics Command/I. Pratt (AMSEL KL-1B)

Fabricate Pyroceram Anatomical Torso

Corning Glass Works
Advanced Products Division
Corning, New York 10008
Contract DAAG17-70-C-0142
Army Natick Laboratories

Research and Development Study on Carbon Fiber Reinforced Bearing Structures
AVCO Corporation
Systems Division
Lowell, Massachusetts 01851
Contract DAOAG-70-C-0040
Army Materials & Mechanics Research Center

PROPERTIES

Research to Investigate the Properties and Structure of Refractory Ceramics, Metals, and Alloys
University of Cincinnati Research Foundation
Cincinnati, Ohio 45221
Contract F33615-70-C-1407 (continuation of F33615-67-C-1178)
Air Force Materials Laboratory/J. W. Poynter (MAMS)

Investigation of Microstrain Properties of Telescope Mirror Materials
Stanford Research Institute
Menlo Park, California 94025
Contract NAS1-9982
NASA, Langley Research Center

Research Hardening of Thermal Oxides on Silicon Via Ion Implantation
Research Triangle Institute
Research Triangle Park, North Carolina 27709
Contract NAS1-10012
NASA, Langley Research Center

Holographic Characterization of Ceramics
TRW, Inc., TRW Systems Group
Redondo Beach, California 90278
Contract N00019-70-C-0136 (continuation of N00019-69-C-0228)
Naval Air Systems Command

Research on Dynamic Response and Adhesion Failures of Rain-Erosion-Resistant Coatings
Hydronautics, Inc.
Laurel, Maryland 20810
Contract N00019-70-C-0276
Naval Air Systems Command

Investigation, Including a Testing Program, on the Influence of Material Variables on Fatigue Mechanisms in Composites
IIT Research Institute
Chicago, Illinois 60616
Contract N00019-70-C-0378
Naval Air Systems Command

Investigate the Strength Characterization of Ceramic Sonar Rings
Stanford Research Institute
Menlo Park, California 94025
Contract N00024-70-C-12244
Naval Ship Systems Command/C. A. Clark (Code 00V1D2)

TEST METHODS

Study, Investigate, and Develop Techniques Necessary to Establish Screening Procedures to Insure the Reliability of Ceramic Multilayer Boards
Sylvania Electric Products, Inc.
Semiconductor Division
Waltham, Massachusetts 02154
Contract F30602-70-C-0212 (continuation of F30602-68-C-0243)
Rome Air Development Center/D. W. Calabrese

Design Study for High-Sensitivity Graphite Crystal Spectroscopy
Columbia University
New York, New York 10027
Contract NAS5-21292
NASA, Goddard Space Flight Center

FUNDAMENTAL BEHAVIOR

Research on Fracture of Composites
Midwest Research Institute
Kansas City, Missouri 64110
Contract N00014-70-C-0212
Office of Naval Research/B. A. MacDonald

Study of the Structural Behavior of Thin Films on Substrates
American Science and Engineering, Inc.
Cambridge, Massachusetts 02142
Contract NASw-2001
NASA, Headquarters

Zirconium Carbide-Graphite Composite Studies
McDonnell-Douglas Corporation
Huntington Beach, California 92647
Contract SNPC-67
Space Nuclear Propulsion Office

DIGEST OF SELECTED ACCESSIONS

INDEX

KEY TERMS	ACCESSION NUMBER
Material:	
Borides	4037, 4337
Carbides	4337
Carbon/graphite	4337, 6179-2, 6298-1, 6935, 6960, 6961
Nitrides	
Oxides (single)	4337, 6124-2, 6898, 6925, 6938, 6939, 6962
Oxides (mixed)	5265-6, 5375-2, 6026-6, 6688-1, 6894, 6923, 6924, 6925, 6936
Silicides	
Sulfides	6924
Selected glasses	6879, 6923, 6954, 6963
Glass-Ceramics	
Intermetallics	4337, 6924
Metalloid elements – B, Si, Ge	6026-6, 6925
Miscellaneous metalloid compounds	6924, 6925
Cermets	
Form:	
Filament	5375-2, 6124-2, 6179-2, 6298-1, 6879, 6898, 6963
Foam	
Single crystal	5375-2, 6026-6, 6124-2, 6898
Composite	4337, 6298-1, 6898
Coating	4337, 5265-6, 6298-1, 6898
Thin film	
Area of Study:	
Applications	4037, 4337, 5265-6, 5375-2, 6026-6, 6124-2, 6179-2, 6298-1, 6688-1, 6894, 6898, 6924, 6936, 6954, 6960
Processing	4037, 5265-6, 5375-2, 6026-6, 6124-2, 6179-2, 6298-1, 6688-1, 6898, 6936, 6962, 6963
Properties	4037, 4337, 5265-6, 5375-2, 6026-6, 6124-2, 6179-2, 6298-1, 6688-1, 6898, 6923, 6924, 6925, 6935, 6938, 6939, 6954, 6960, 6961, 6962, 6963
Test Methods	5265-6, 5375-2, 6026-6, 6124-2, 6179-2, 6298-1, 6688-1, 6898, 6935, 6939, 6960, 6961, 6962
Fundamental behavior	4037, 4337, 6026-6, 6688-1, 6923, 6924, 6925, 6935, 6938, 6954
Information analysis	6879

Although DCIC cannot supply copies of the documents listed in this section, it will render all possible assistance to identify the appropriate sources for such copies.

DIGESTS

4037 Oxidation-Resistant Diborides

ManLabs has conducted an intensive development and evaluative program on diboride materials containing either ZrB_2 or HfB_2 as the principal component with selected additives to enhance oxidation resistance, mechanical properties, and thermal-stress resistance. The materials employed in this study are listed in Table 4037-I.

TABLE 4037-I. DIBORIDE MATERIALS EVALUATED

Hafnium Diboride Materials*	Zirconium Diboride Materials*
HfB_2	ZrB_2
95HfB_2· 5SiC	90ZrB_2·10SiC
80HfB_2·20SiC	80ZrB_2·20SiC
70HfB_2·30SiC	95ZrB_2· 5C(filament)
HfB_{2+}-SiC	80ZrB_2·20C
80HfB_2·20C	50ZrB_2·50C
50HfB_2·50C	72ZrB_2·18SiC-10C
56HfB_2·14SiC-30C	56ZrB_2·14SiC-30C
80HfB_2·20HfSi	90ZrB_2·10SiB_6
96HfB_2· 4Hf-Ta	80ZrB_2·20SiB_6
	92ZrB_2· 8Cr
	ZrB_2· W

*Base compositions in volume percent, where given.

The voluminous data generated in the program, so far, are given in the eight reports listed below. Some of the pertinent conclusions of the program are as follows:

(1) Manufacturing capability is available within present powder-production technology to produce ZrB_2 powder in 100 to 400-pound quantities which meets specifications developed in this program for hot-pressing grades to be employed with SiC and/or C additives. Production capability for HfB_2 powder is not similarly advanced as demonstrated by variability from lot to lot of 50 to 100-pound quantities. Limited availability of hafnium oxide of suitable composition as a starting material for production of HfB_2 and apparent reaction variability in the production process contribute to procurement difficulties of HfB_2.

(2) The additives, SiC and/or C, function to enhance the hot-pressing characteristics of ZrB_2 and HfB_2 powder by lowering the fabrication temperature needed to consolidate the powders to full densification. The additives employed in suitable quantities also provide a grain-size control, eliminate processing difficulties encountered in the processing of ZrB_2 and HfB_2 with no intentional additives, and increase the physical integrity of the material. Polycrystalline diboride composite materials comprised of ZrB_2 with discrete particles of SiC and/or C can be hot pressed in sizes up to 6 inches square by 2 to 3 inches high without reduction in properties or performance as obtained from 2 and 3-inch-diameter billets, provided adequate mixing is achieved and proper modifications of processing cycles are employed. Nondestructive testing procedures are available for assessing material integrity and variability. Hot pressing of hollow cylindrical shapes of the composite materials of 4 to 6 inches OD by 3 to 5 inches ID by 4 to 6 inches high appears feasible for production of dense structures. The larger sized billets could also be fabricated with HfB_2 base compositions providing suitable diboride powder was procured.

(3) Present hot-pressing technology and powder-production capability are adequate to extend the sizes of billets fabricated and the quantities of ZrB_2 procured to 8-inch-diameter by 4-inch-high billets and 500 to 1000-pound powder lots. The system of ceramic additives provides fabrication enhancement such that processing of shaped billets other than cylinders should be attainable if moderately simple shapes of near uniform thickness are desired.

(4) The relative amounts of the base-metal diboride, silicon carbide, and carbon can be adjusted to provide the maximum oxidation resistance which is imparted by the diboride and silicon carbide while maintaining mechanical properties and thermal-stress resistance which are controlled by the silicon carbide and the carbon; the carbon detracts somewhat from the oxidation resistance.

(5) The oxidation resistance of the base-metal diboride is not affected by the presence of 5 to 10 volume percent of ceramic impurities such as the base-metal carbide or oxide, boron carbide or free graphite.

(6) Thermochemical stability of the diboride composite materials in hot-gas/cold-sample tests in oxidizing atmospheres is provided by a combination of the protective oxide which forms from the base-metal diboride and the oxides of silicon and carbon. The oxides function to thermally insulate the base diboride material from the hot-gas atmosphere. As the temperature of the oxide increases, the more volatile oxides are preferentially lost and the exterior oxide is effectively the metal oxide with the material limiting temperature being the melting point of the metal oxide.

(7) The system of ceramic additives comprised of SiC and/or C developed, employed with ZrB_2 or HfB_2, produce hot-pressed, dense, sound materials of substantially improved mechanical properties without significantly reducing thermal stability or oxidation resistance.

(8) Additions of SiC do not materially affect the elastic modulus of ZrB_2 or HfB_2; additions of C or porosity decrease the elastic modulus by somewhat larger amounts than predicted by theoretical calculations.

(9) The relative amounts of the base-metal diboride, silicon carbide, and carbon can be adjusted to provide a maximum strength-to-elastic modulus and strength-to-density ratios without sacrificing thermal stability or oxidation resistance.

(10) The presence of carbon in amounts of 10 to 30 volume percent produces strength anisotropy in hot-pressed billets. Materials parallel with the plane of the billet (perpendicular to the hot-pressing direction) have bend strengths greater than materials perpendicular to the plane of the billet. (The 10 volume percent is not a lower limit; data for structures with less than this amount were not obtained.)

(11) The presence of carbon as agglomerates or perhaps discrete particles can effect a crack-arrestment phenomena at elevated temperatures.

(12) Deformation rates are inversely proportional to grain size and proportional to the 0.4 power of strain rate. Higher deformation rates observed for $80ZrB_2 \cdot 20SiC$ (7 to 10 microns) versus ZrB_2 (18 to 23 microns) are consistent with the grain size of the structures tested. Grain-boundary sliding is considered to be the dominant deformation mechanism for both materials, and scanning-electron-microscope studies supported this view.

(13) The grain-size stabilization and the presence of SiC in zirconium diboride materials (and presumably in HfB_2 analogs) impart a strain-hardening capacity which could prove useful as a design consideration for long-term or cyclic applications. A "degree of toughness" develops in $ZrB_2 \cdot SiC$ materials (and presumably in HfB_2 analogs) at elevated temperatures as demonstrated by a stress drop (due to the deformation processes) prior to the onset of failure.

SELECTED ACCESSIONS

(14) Hot-pressed diboride compositions containing ZrB_2 or HfB_2 as the principal component with up to 20 to 34 volume percent total addition of SiC and/or C possess high thermal conductivities at room temperature of the order of 0.20 cal cm/cm^{2}sec C. The compositions also display high values at 2000 C of the order of 0.10 cal cm/cm^{2}sec C.

(15) The diboride compositions displayed metallic-like electrical resistivity at room temperature and positive temperature coefficients. Variations of composition and porosity can be used to produce materials with varying room-temperature resistivities and temperature coefficients.

(16) The total normal emittance of the unoxidized diboride compositions is higher than observed for the oxidized materials which show values of 0.60.

(17) The diboride compositions displayed a level of thermal-stress resistance in a controlled steady-state laboratory test which is unsurpassed by any other ceramic material. The onset of plastic deformation and resultant stress relief at temperatures of 1000 to 1800 C, dependent upon strain rate and stress, affects the thermal-stress resistance and the analysis of thermal-stress data. Proper assessment of the latter must include provisions to account for deviations from totally elastic behavior.

(18) The diboride compositions hot pressed with SiC and/or C additives can be employed to provide dense sound materials which are excellent candidates for the nose caps and leading edges of hypersonic high L/D reentry vehicles and can be considered for multiple reuse applications.

(19) Heat-transfer and thermal-stress analyses predict that leading configurations of diboride composition ZrB_2-SiC-C can sustain stresses introduced in currently considered trajectories.

(20) Diboride materials are potential candidates for air-inlet leading edges of engines for hypersonic vehicles; additional characterization data for this application are required.

(21) Diboride materials are excellent candidates for nozzle-throat inserts and other hardware for rocket motors which employ hydrazine and nitrogen tetroxide type fuel mixtures.

Research and Development of Refractory Oxidation-Resistant Diborides, AFML-TR-68-190, ManLabs, Inc., Contract No. AF33(615)-367

Part I, E. V. Clougherty, D. Kalish, and E. T. Peters (July, 1968) (287 pages, 77 tables, 143 figures) AD 839 956.

Part II, Volume I, "Summary", E. V. Clougherty (1970) (84 pages, 19 tables, 19 figures).

Part II, Volume II, "Processing and Characterization", E. V. Clougherty and E. T. Peters/R. J. Hill and W. H. Rhodes, AVCO Corp. (January, 1970) (180 pages, 53 tables, 74 figures) AD 866 558.

Part II, Volume III, "Thermochemical Stability Characterization", E. V. Clougherty and E. T. Peters (January, 1970) (143 pages, 19 tables, 78 figures) AD 866 155.

Part II, Volume IV, "Mechanical Properties", W. H. Rhodes, AVCO Corp., E. V. Clougherty and D. Kalish (January, 1970) (137 pages, 16 tables, 78 figures) AD 865 809.

Part II, Volume V, "Thermal, Physical, Electrical, and Optical Properties", E. V. Clougherty/K. E. Wilkes and R. P. Tye, Battelle Memorial Institute (November, 1969) (81 pages, 14 tables, 49 figures) AD 865 321.

Part II, Volume VI, "Thermal Stress Resistance", E. V. Clougherty/D. E. Niesz, Battelle Memorial Institute/A. L. Mistretta, Bell Aerosystems Company (December, 1969) (75 pages, 15 tables, 21 figures) AD 865 322.

Part II, Volume VII, "Application Evaluations and Design Considerations", E. V. Clougherty/F. M. Anthony, Bell Aerospace Company (March, 1970) (127 pages, 24 tables, 42 figures).

Part III (Additional Fabrication and Evaluation Studies), not yet released.

4337 Refractory Materials Versus High-Velocity Atmospheric-Flight Conditions

The response of refractory materials to oxidation in air over a wide range of time, gas velocity, temperature, and pressure has been studied in a multidisciplinary program conducted by ManLabs for the Air Force (AFML). The study spans the heat flux and boundary-layer-shear spectrum of conditions encountered during high-velocity atmospheric flight, as well as conditions normally employed in materials-oriented investigations. Efforts were made to elucidate the relationship between hot-gas/cold-wall (HG/CW) and cold-gas/hot-wall (CG/HW) surface effects in terms of heat- and mass transfer rates at high temperatures, so that full use could be made of both types of experimental data.

Exposures of specimens in HG/CW tests were performed in AVCO facilities which provided stagnation pressures between 0.002 and 4.0 atmospheres, stagnation enthalpy between 2000 and 16,000 Btu/lb, cold-wall heat flux between 100 and 1500 Btu/ft^2 sec, and exposure times between 20 and 23,000 seconds. Exposure tests also were conducted in the Cornell Wave Superheater which provided heat flux leads up to 8000 Btu/ft^2 sec at very high gas velocity for short time. The CG/HW tests included (1) specimens heated in furnace with air flowing at 0.9 to 9.0 ft/sec for times from 5 minutes to 4 hours, (2) specimens heated by induction in oxygen-helium mixtures at flow rates of 0.2 ft/sec and oxygen partial pressures of 0.013 to 0.20 atmosphere for times up to four hours, and (3) specimens heated inductively (2000-4500 F) with air-flow rates between 10 and 300 ft/sec for times up to 1 hour.

The materials evaluated in the program are listed in Table 4337-I.

TABLE 4337-I. REFRACTORY MATERIALS EVALUATED

Boride Materials	Carbon Materials	
$HfB_{2.1}$	RVA	
ZrB_2	PG	
HfB_2 + 20 v/o SiC	BPG	
Boride Z		
$HfB_{2.1}$	PT 0178	
$HfB_{2.1}$ + 20 v/o SiC	POCO (AXF-5Q)	
$ZrB_{2.1}$ + 20 v/o SiC	Glassy Carbon	
$HfB_{2.1}$ + 35 v/o SiC	JTA	
ZrB_2 + 14 v/o SiC + 3 v/o C	JT 0992	
	JT 0981	
Carbide Materials	**Coated Materials**	
HfC + C	Si/graphite	
ZrC + C	Ir/graphite	
	Sn-Al/Ta-W	
	WSi_2/W	
Oxide Materials	**Metallic Alloys**	
SiO_2 + 68.5 w/o W	Hf-20Ta-2Mo	Ir-Pt
SiO_2 + 60 w/o W	W-Ag	Ir-Rh
SiO_2 + 35 w/o W	W-Zr-Cu	Ir-Re
	Ir	Ir-Os

Pretest material characterization and posttest examination were made on the candidate materials. The specimens ranged from 0.5 to 1.5 inch in diameter.

Some of the major accomplishments of the program include:

(1) Delineation of the altitude-velocity/flux-enthalpy comparison for refractory materials

(2) Demonstration of the reuse capabilities of boride composites for multimission lifting reentry trajectories

(3) Identification of the minimum oxide temperature limit criteria for HG/CW performance

(4) Measurement of temperature gradients through oxide films during HG/CW and high-velocity CG/HW tests

(5) Calculation of temperature gradients through oxide films in HG/CW tests

(6) Specification of low-temperature failures in refractory materials

(7) Effects of pressure on the oxidation behavior of refractory materials

(8) Observations of thermal-stress failures

(9) Effects of sample orientation on the thermal-stress resistance of hot-pressed materials

(10) Measurement of spectral and total normal emittance under oxidizing conditions

(11) Prediction of model surface temperature from stream conditions

(12) Prediction of 1 to 3-mil-per-second-boundary based on melting

(13) Effects of cyclic exposure under oxidizing conditions

(14) Effects of alloying and oxide additions on the oxidation of iridium alloys

(15) Influence of sample geometry and air-flow rate on graphite oxidation kinetics

(16) Influence of calorimeter and shroud size and shape on the measured heat flux

(17) Formulation and programming of generalized surface-reaction problem

(18) Calculation of graphite ablation rates.

Details of the program and results obtained are covered in the various reports listed below.

Stability Characterization of Refractory Materials Under High Velocity Atmospheric Flight Conditions, AFML-TR-69-84, ManLabs, Inc., Contract No. AF 33(615)-3859:

Part I, Volume I, "Summary", L. Kaufman and H. Nesor (March, 1970) (83 pages, 7 tables, 47 figures).

Part II, Volume I, "Facilities and Techniques Employed for Characterization of Candidate Materials", L. Kaufman and H. Nesor (December, 1968) (86 pages, 23 tables, 68 figures) AD 865 317.

Part II, Volume II, "Facilities and Techniques Employed for Cold Gas/Hot Wall Tests", L. Kaufman and H. Nesor (December, 1969) (55 pages, 2 tables, 41 figures) AD 864 968.

Part II, Volume III, "Facilities and Techniques Employed for Hot Gas/Cold Wall Tests", L. Kaufman and H. Nesor (December, 1969) (122 pages, 10 tables, 78 figures) AD 865 316.

Part III, Volume I, "Experimental Results of Low Velocity Cold Gas/Hot Wall Tests", L. Kaufman and H. Nesor (December, 1969) (118 pages, 19 tables, 103 figures) AD 865 319.

Part III, Volume II, "Experimental Results of High Velocity Cold Gas/Hot Wall Tests", R. Perkins (Lockheed Missile/Space Company), L. Kaufman and H. Nesor (December, 1969) (125 pages, 17 tables, 82 figures) AD 865 323.

Part III, Volume III, "Experimental Results of High Velocity Hot Gas/Cold Wall Tests", L. Kaufman and H. Nesor (February, 1970) (336 pages, 39 tables, 349 figures).

Part IV, Volume I, "Theoretical Correlation of Material Performance with Stream Conditions", L. Kaufman, H. Nesor, H. Bernstein, and J. R. Baron (December, 1969) (115 pages, 28 tables, 48 figures).

Part IV, Volume II, "Calculation of the General Surface Reaction Problem", H. Bernstein and J. R. Baron (December, 1969) (144 pages, 22 tables, 23 figures).

Part V, Volume I (Additional Materials Evaluations), not yet released.

5265-6 Thermal Control Coatings

Results of the in situ optical spectroscopy of ultraviolet-irradiated, reactively encapsulated (surface treated) zinc orthotitanates (Zn_2TiO_4) are discussed in this report by IIT Research Institute. This investigation is part of a broader research effort directed at the development of thermal-control surface coatings that possess very low but stable ratios of solar absorptance to infrared emittance.

The most important factor influencing the achievement of optical stability (relative to ultraviolet irradiation) with Zn_2TiO_4 is the use of excess (~0.5 percent) ZnO in the preparative reaction, although surface treatments (such as plasma annealing or application of potassium silicate, sodium acid phosphate, and iron cyanide) are also important in this respect. Residual ZnO must be present when any high-temperature heat treating is performed. Silicating (and preparation of potassium silicate-based coatings) is the most effective surface treatment for improving the stability of Zn_2TiO_4.

Irradiation at high temperature (e.g., 165 C) caused severe damage to silicate and silicone paints prepared with Zn_2TiO_4, due primarily to the formation of Ti^{3+}. Powders exhibited greater resistance to damage by high-temperature irradiation.

Development of Space Stable Thermal Control Coatings, G. A. Zerlaut and N. A. Ashford, IIT Research Institute, Contract No. NAS8-5379 (February, 1970) (44 pages, 24 figures).

5375-2 Dielectric Ceramics

This report discusses the results of a study of ceramic dielectric materials at Rutgers University intended "to determine the principles, mechanisms, and techniques by which ceramics can be made to approach their ultimate properties or some desired, specific properties". The specific objectives of the research are:

(1) To develop low-loss, voltage-controlled, nonlinear dielectrics for use at cryogenic temperatures in voltage controlled, tuneable, superconductive RF networks

(2) To develop dielectric ceramics possessing a dielectric constant greater than 90, a temperature coefficient of dielectric constant

under 40 ppm/C over the temperature range -40 to +85 C, and a dissipation factor less than 0.0003 at 1 to 10 GHz

(3) To evaluate the utility of new or novel techniques for producing or processing materials having unusual or specifically desired properties. [Thin flakes (~0.2μ thickness) and fine fibers (0.75 to 2μ diameter) of glasses which host a ferroelectric crystalline devitrification phase are being studied; the effect of prior chemical treatment of the powder on the fired properties of barium titanate ceramics is being investigated.]

The materials studied as nonlinear low-loss, voltage-variable dielectrics include single-crystal $SrTiO_3$, polycrystalline $SrTiO_3$, and polycrystalline $BaTiO_3$ containing $SrSnO_3$. Electrical-property measurements were made over the temperature range 3 to 298 K.

Measurements of the voltage variability of the $BaTiO_3$ + 9 percent $SrSnO_3$ solid solution show that voltage variability increases near the Curie point in agreement with literature on other materials undergoing a ferroelectric-paraelectric transition. Initial results of electrical testing of single-crystal and polycrystalline $SrTiO_3$ specimens are presented. The peak in the Q versus temperature curve reported by other investigators was observed. At 77 K a single-crystal specimen of $SrTiO_3$ exhibited a 1.7:1 decrease in dielectric constant when d-c bias of 74 v/mil was applied. The field caused a large drop in Q, going from 570 at zero bias to 40 at 74 v/mil.

One phase of the development of low-loss microwave ceramics has been pursued through compositional studies in the $BaTiO_3$-$CaZrO_3$-Fe_2O_3 system. $BaTiO_3$ contents were varied from 81 to 91 mole percent, $CaZrO_3$ from 9 to 11 percent, and Fe_2O_3 from 0.75 to 2.0 percent. Dielectric constants and dissipation factors obtained at 1 KHz were in the ranges of 1500 to 2000 and 0.02 to 0.005, respectively. Over the temperature range -40 to +95 C, temperature coefficients of dielectric constant (TC_K) were all negative. The lowest TC_K obtained was -938 ppm/C with a variation in K of +0 and -11.2 percent. These were the lowest values achieved in this work over the entire temperature range of -40 to +85 C with materials having low dissipation factors.

Another approach to the development of low-loss microwave ceramics that is under investigation is the preparation of layered ceramics using two compositions whose series capacitance results in a near-zero dependence of dielectric constant on temperature. Compositions in the $BaTiO_3$-$SrSnO_3$ system were prepared for use as end members in this work. These compositions were produced both by simply ball milling and by milling followed by prereaction. The prepared end members were then fabricated into specimens using both layering and superficial mixing techniques. Specimens were sintered by both conventional and hot-pressing techniques. Results obtained to date indicate that hot pressing has the greatest potential for producing layered dielectric ceramics with the desired properties.

Chemical-treatment techniques developed for upgrading barium titanate powders consisted of chemically treating the raw particulate with acetic acid, ammonium hydroxide, or distilled water. Specimens prepared from treated raw materials sintered to approximately the same bulk density as untreated material and exhibit an increase in dielectric constant to approximately 4400. Tan δ was essentially unaffected by the chemical treatment.

Inorganic Dielectrics Research, E. J. Smoke, et al, Rutgers University, Contract DAAB07-69-C-0109, Report No. ECOM-0109-1 (February, 1970) (79 pages).

6026-6 Spinel for Electronic Applications

Research at RCA is intended to lead to the utilization of magnesium aluminate spinel as substrate material in epitaxial-silicon integrated electronics. The advantages of spinel over sapphire (the conventionally used substrate material) include:

(1) less hardness for surface preparation

(2) less auto doping to silicon

(3) more compatible thermal expansion and lattice match with silicon

(4) unique epitaxial relationship

(5) selectable orientation and composition for optimization.

In the current investigation, emphasis was placed on spinel crystal growth by the seeded growth technique and on the surface preparation for substrate surface.

Low Al-rich spinel crystals were successfully grown on (100) seeds using feeds of the same composition. Epitaxial silicon films (p-type) grown on spinel substrates prepared from the seed-grown crystals of good quality exhibit mobilities equal to or near the bulk values. The defect structures of Verneuil-grown spinel crystals were examined by various techniques. The two main defects are the formation of cracks after growth or during cutting, and the presence of subgrains in the crystals. The mechanical stability of the crystals, after postgrowth annealing, was found to be significantly improved.

The thermal-expansion, dielectric, and optical properties of low Al-rich spinel crystals were determined. The thermal-expansion coefficient of the low Al-rich spinel is less than that of the stoichiometric spinel. The dependence of dielectric constant on composition for spinel is very slight. The Verneuil-grown spinel crystals exhibit characteristic absorption bands in the infrared region, and this property is useful to determine the spinel composition.

Surface preparation of the spinel substrates using hydrogen halides as the gas etchants was studied. It was found that the halides are not suitable for polishing spinel. New polishing compounds were explored for mechanical polishing of spinel surface. Preliminary results indicate that a ZrO_2-containing compound may be a potential polishing agent to yield a scratch-free spinel substrate surface.

The quality of epitaxial silicon grown on spinel was studied. Both the effect of substrate bulk crystalline perfection and the effect of substrate surface preparation were determined. Deposition of silicon on spinel using the H_2 reduction of $SiCl_4$ process was investigated. This process may be advantageously used when the spinel substrate is covered initially with silicon grown by the silane process.

Silicon-on-spinel MIS structures were fabricated using p-type silicon and vapor-phase deposited Al_2O_3 and Si_3N_4 as the passivating dielectrics. Optimization of the processing parameters was determined and an electrical evaluation was performed on the MIS structures.

Single-Crystal Spinel for Electronic Application, C. C. Wang, et al, RCA Laboratories, Contract No. F33515-69-C-1073, Report No. AFML-TR-69-315 (February, 1970) (73 pages, 15 tables, 39 figures).

6124-2 Whisker-Reinforced Piezoelectric Ceramics

Tracor has reported the results of a study to determine the efficacy of whisker reinforcement regarding improvement in the tensile strength of piezoelectric ceramics. The objective of the work was to develop an improved ceramic piezoelectric for use in high-power sonar transducers. The results reported were obtained on sapphire whisker (18 and 0.5-μ diameter; 60/1 and 25/1 aspect ratios) composites of lead zirconate titanate (LZT) or barium titanate matrix.

Whisker composites (5-10 v/o whisker) were cold pressed, bisque fired in air at 750 C, then sintered in lead oxide atmosphere (LZT composite) or air (barium titanate composite) at 1290 to 1320 C. Fired composite specimens were examined to determine density, dielectric constant, modulus of rupture (on 1/8 x 1/8 x 1-inch beams), impact resistance, and microstructural characteristics.

LZT composites containing 10 v/o sapphire whiskers were produced having a dielectric constant (unpoled) of 700 to 800 and an impact strength roughly twofold greater than that of the unreinforced matrix. The dielectric constants and plate coupling coefficients of the composite specimens were 40 percent lower than those of the unreinforced matrix. Best results were obtained with the 0.5-μ whisker reinforcement.

Structurally sound barium titanate composites containing sapphire whiskers could not be produced.

Whisker Reinforcement of Piezoelectric Transducer Ceramics, R. R. Whymark and K. J. Triebes, Tracor, Contract No. N00014-68-C-0325 (January, 1970) (36 pages, 5 tables, 6 figures).

6179-2 Graphite for Reentry Applications

Processing studies and preliminary material-characterization data are described for three-dimensionally reinforced carbon/carbon composites. Experiments in which yarns were woven in 4, 5, and 7 directions were performed. Three-dimensional composites in which both PAN and rayon precursor yarn were woven in 4 directions were fabricated using 150 C (softening point) pitch or a mixture of 150 C pitch with another material. Mechanical and thermophysical properties were determined. The conclusion is that anisotropy limits the applications of this material. For example, the tensile strength was shown to decrease from about 9000 psi along a fiber direction to about 2000 psi at 50 degrees to the fiber. The large thermal-expansion anisotropy and distortions experienced during thermal processing were also serious disadvantages. It is recommended that the unidirectional 3-D composites would be improved by using smaller diameter, more isotropic reinforcements and stronger, more isotropic binder matrices.

A separate task within this program sought to develop an improved binder matrix from pitch by use of additives. Both No. 1512 pitch (softening point, 87 C) and a 150 C (softening point) pitch were used. Additives included sulfur, $FeCl_3$, phenolic resin, furane resin, epoxies, polyacrylonitrile, acrylic resins, and polyamide. Coking-value studies showed that the already high coking value of the 150 C pitch was not affected significantly by any of the additives. Further, it was concluded that the impregnating qualities of the 150 C pitch were not improved upon by any of the additives investigated.

Ablation studies on four-directional, 3-D composite of rayon and PAN precursor yarns indicate that the rayon precursor carbons were preferentially etched from the pyrolytic carbon matrix material whereas the PAN carbons were left in relief. This is taken to mean that the PAN carbons are more resistant to oxidation than rayon carbons.

Improved Graphite Materials for Re-Entry Vehicles, E. R. Stover, General Electric, Contract No. F33615-68-C-1283, Report No. AFML-TR-69-67, Vol III (April, 1970) (142 pages, 16 tables, 122 figures).

6298-1 Graphite-Filament Reinforced Plastics

Philco-Ford is investigating the use of graphite filaments as reinforcements for advanced composites. Small, flexible filaments in yarn or tow form are prepared by pyrolyzing rayon or polyacrylonitrile to an oriented graphitic crystalline condition. The advantages of graphite over fiber glass are much higher modulus and lower specific gravity. The advantages of graphite over boron filament are greater flexibility for applications involving complex shapes and small-radius bends, lower specific gravity, and, potentially, a much lower price.

Current work was directed at improving the performance of high-modulus graphite-filament reinforced composites with particular emphasis on improvements in the interfacial bond between the filaments and resin binders. Evaluation of the unidirectional and bidirectional composite properties was made using static tensile, compressive, and shear-strength measurements. Four high-temperature, thermosetting resin systems were used in composite preparation.

A pyrolytic carbon coating deposited on the graphite fibers, prior to resin impregnation, improved the fatigue resistance of unidirectional and bidirectional composites and increased shear strength and tensile strength of unidirectional composites. No increase in unidirectional compressive strength or transverse strength was obtained by use of the coating. Translaminar cracking in bidirectional composites, observed after heat curing, was reduced by maintaining pressure on the composites during the entire cure and cooling cycle, by increasing the fiber volume or by using a more resilient binder.

A polyimide resin and a polyquinoxaline resin, combined into graphite-reinforced composites, had excellent resistance to thermal degradation in 300 C nitrogen. Both types of composites degraded in 300 C air, but the polyquinoxaline was superior. Both binders appear to have lower adhesion to graphite fibers than epoxy resin. The polyquinoxaline was difficult to process while the polyimide was relatively easy to use.

Analysis of compressive failures in flexure specimens indicated that compressive failure in the composites was governed by the fiber strength. The fiber-to-matrix adhesion appeared to be a less important factor.

Graphite Filament Reinforced Plastics, N. E. Quackenbush and D. R. Doner, Philco-Ford Corporation, Contract No. N00019-69-C-0135 (January, 1970) (72 pages, 14 tables, 24 figures).

6688-1 Microwave High-Dielectric-Constant Ceramics

Raytheon researchers describe their efforts to develop ceramic dielectric materials for microwave applications having the following properties over the 1 to 10-gigahertz range:

(1) $25 < k < 35$

$|\tau| < 50$ ppm/C -40 to 85 C

$\tan\delta < 3 \times 10^{-4}$

(2) $40 < k < 80$

$|\tau| < 50$ ppm/C -40 to 85 C

$\tan\delta < 3 \times 10^{-4}$,

where k is the dielectric constant and τ is the temperature coefficient of the dielectric constant, $\tau = 1/K^{dk}/dT$.

Over 200 samples of 20 ceramic oxide compounds were investigated. Dielectric properties were measured at 1 MHz and at X-band. Dielectric properties also were measured at microwave frequencies below X-band using a radial dielectrometer. Compacts of the compounds were prepared by both conventional dry-press-and-firing techniques and hot-pressing techniques.

The most promising materials for microwave-device applications and their properties (at 20 C) were:

(1) $BaTi_4O_9$:k = 37.9, tanδ = 6.5 x 10^{-4},
τ = -65 ppm/C

(2) lithium titanate:k = 25.7, tanδ = 2.6 x 10^{-4},
τ = -40 ppm/C .

No materials were found which appear to be suitable for the attainment of dielectric constants in excess of 40 which fulfill the additional desired property requirements.

Microwave High Dielectric Constant Materials, D. W. Ready, et al, Raytheon Company Research Division, Contract No. DAAB-07-69-C-0455 (March, 1970) (50 pages, 15 tables, 12 figures).

6879 Glass-Vapor Interactions

A literature survey has been prepared by workers at the Engineering Research Institute of Iowa State University covering the published investigations of the nature of the surfaces of inorganic glasses and the interaction of glasses and various adsorbates. The literature included in the survey spans the time period from 1949 to 1969.

Topical sections of the abstracted bibliography include (1) properties of glass (e.g., strength, as affected by environmental factors), (2) glass structure, including surface morphology and porosity characteristics, (3) properties of adsorbates, mainly data on adsorbed water, (4) adsorption of vapors on glass, (5) phenomenological aspects of adsorption of gases or solids, (6) thermodynamic properties of adsorbate-adsorbent systems, surface and interfacial energies, (7) measurement of contact angle, adhesion, and wettability, (8) interaction between inorganic glasses and organic resins, and (9) infrared spectrographic studies of glass.

A total of 233 technical articles and patent disclosures are contained in the survey.

A Literature Survey on Physicochemical Properties of Glass Surfaces and Their Interaction with Vapors, R. J. Huang, R. D. Johnson, T. Demirel, T. D. McGee, Engineering Research Institute, Iowa State University, Project 713-S, Contract No. F33615-68-C-1034 (February 1970) (109 pages).

6894 Controlled-Microstructure Ceramics

The United Aircraft Research Laboratories has begun work on a study of the preparation of ceramics of eutectic composition in which the microstructure has been controlled by unidirectional solidification. This investigation is patterned after similar work with eutectic metal systems which demonstrated that in situ growth of dispersed fiber or platelet phases in a solidifying eutectic resulted in a conveniently prepared composite with superior mechanical properties.

The report covers the first year of a proposed 3-year program. The initial laboratory study was done on 29 binary oxide systems; most with a eutectic temperature below 1000 C.

Four different pieces of equipment were assembled for unidirectional-solidification experiments. Most of the experiments were conducted using a modified Bridgman-Starkbarger solidification furnace in which it was possible to maintain a high liquid-solid temperature gradient independent of ingot length. In the device, water is continually sprayed on the outside of an alumina tube containing the melt as it is slowly lowered from a Pt-Rh wire wound furnace. The rate of solidification varied from 0.5 to 5.0 cm/hr.

Ingots of the 29 eutectic compositions were examined using transmitted light microscopy techniques. It was estimated that nine of the systems studied exhibited good potential regarding the controlled growth of a lenticular phase within a solidifying matrix. These included the systems $PbO\text{-}Fe_2O_3$, $PbO\text{-}Nb_2O_5$, $Bi_2O_3\text{-}ZnO$, $Bi_2O_3\text{-}Fe_2O_3$, $CaO\text{-}WO_3$, $SrO\text{-}WO_3$, $MgO\text{-}WO_3$, $Fe_2O_3\text{-}La_2O_3$, and $Fe_2O_3\text{-}Y_2O_3$.

Effect of Eutectic Microstructure on the Properties of Ceramic Oxides, C. Hulse and J. Batt, United Aircraft Research Laboratories, Project No. NR032-516, Contract No. N00014-69-C-0073 (March, 1970) (34 pages, 2 tables, 14 figures).

6898 Metal-Matrix Composites

Work has been under way at the General Electric Space Sciences Laboratory since 1960 to develop composite materials for high-temperature applications by reinforcing metals with high-strength ceramic whiskers or fibers. The objective of the most current phase of this program is to develop Al_2O_3-filament reinforced nickel-based composites with strength-to-density ratios of 200,000 inches at temperatures in excess of 1100 C.

A suitable fabrication procedure, based on hot pressing arrays of coated sapphire filaments between nickel-alloy sheets (0.025-inch thick) was developed. Dense, well-bonded composites were produced by compacting nichrome sheet-sapphire fiber arrays at 6000 psi for 10 to 30 minutes at 1200 C.

The filaments used in preparing the composites were produced as continuous single-crystal sapphire filaments, 0.01 to 0.02 inch in diameter. Tungsten and Y_2O_3 were studied as coating materials for the filaments to minimize adverse reactions between the Al_2O_3 and Nichrome alloy at elevated temperatures. The results of high-temperature (1100 C) tensile-strength and bend-strength studies of hot-pressed composites led the workers to conclude that the concept of using a stable oxide coating (Y_2O_3) to protect sapphire fibers from degradation in a nickel-based-alloy-matrix composite is feasible and should be pursued in future research.

Development of Composite Materials for High Temperature Applications, M. J. Noone, General Electric Company, Final Report, Contract N00019-69-C-0310 (January, 1970) (53 pages, 5 tables, 15 figures).

6923 Glass-Ceramics

This report describes a 3-year study at Owens-Illinois to characterize the high-quartz and keatite solid solutions which occur as important principal microcrystalline phases in glass-ceramic materials. The unique properties of these phases including negative thermal expansion, contribute significantly to the overall properties of glass-ceramic bodies. The primary objective of the research was to determine the structures and chemical compositions of the solid-solution phases, including details of crystal lattice defects in terms of specific order-disorder phenomena on a submicro, domain, or unit-cell scale.

Previous research by the project investigators had shown that certain solid-solution phases in glass-ceramic materials gave rise to X-ray diffraction satellite reflections. The satellite reflections from the high-quartz-type solid-solution $MgO \cdot Al_2O_3 \cdot 3SiO_2$ are especially intense although similar diffraction patterns arise from $MgO \cdot Al_2O_3 \cdot xSiO_2$, where $2 < x < 6$. Single crystals of the 1:1:3 composition were chosen for detailed structure and superstructure studies. It was established that the main and superstructure reflections show hexagonal symmetry. The superstructure reflections in the form of satellites had lead to a thirtyfold superperiod in the c-direction and to a doubling of the a-axes of a high-quartz-like subcell.

High-quartz solid solution of composition $Li_2O \cdot Al_2O_3 \cdot 3SiO_2$ does not give rise to satellite reflections. The crystal structure of $Li_2Al_2Si_3O_{10}$ (high-quartz solid solution) was identified as a stuffed derivative of high quartz. At elevated temperature, this structure ($Li_2O \cdot Al_2O_3 \cdot 3SiO_2$) does not transform into keatite solid solution, although the high-quartz structure of $Li_2O \cdot Al_2O_3 \cdot 4SiO_2$ does transform. Ordering in the high-quartz structures is discussed in terms of atom replacement, e.g., Li or Zn for Mg in the $MgO \cdot Al_2O_3 \cdot 3SiO_2$ high-quartz solid solution.

The crystallization and stability of keatite solid solutions from glasses of base compositions $Li_2O \cdot Al_2O_3 \cdot nSiO$ within n varying from 3.6 to 5.7 was studied as a function of substitution of lithium by magnesium, aluminum by boron, or galium. Almost 50 mole percent Li_2O could be replaced by MgO, although the keatite solid solution thus obtained was not stable and exsolved cordierite at higher heat treatment. At 40 mole percent replacement level, the phase was stable only with $n = 4$, and at 20 mole percent level, it was stable for all the n values investigated. The lower limit of n value ($\simeq 3.6$) for keatite solid-solution formation did not change as a result of the substitution. Mg^{2+} was found to occupy the Li^+ site in the keatite lattice where it causes a greater degree of charge imbalance of the oxygen ions, thus limiting the extent of replacement and thereby affecting the stability of the phase. Stable keatite solid solutions with replacement of aluminum by boron up to about 50 mole percent level were crystallized, even with composition as low as $n = 3$.

Ga_2O_3 could exclusively substitute for Al_2O_3 in a keatite lattice but only for $n > 4$. Glasses with high concentration of galium tended to crystallize phases with galium in sixfold coordination (position, e.g., spinel, α-eucryptite). With $n = 4$, at least 50 mole percent aluminum could be replaced by galium.

SELECTED ACCESSIONS

A detailed crystallographic study was undertaken of the reconstructive transformation:

$$\underset{\text{(high-quartz phase)}}{LiAlSi_2O_6} \rightarrow \underset{\text{(keatite phase).}}{LiAlSi_2O_6}$$

The transformation matrix was first derived from the powder data and then confirmed by single-crystal data.

Characterization of Microcrystalline Phases in Glass-Ceramic Materials, G. M. Muchow, H. Schulz, C. T. Li, S. Ray, Owens-Illinois, Contract No. N00014-67-C-0539 (April, 1970) (220 pages, 13 tables, 12 figures).

6924 Linear Electrooptic Modulator Materials

This EPIC document presents a comprehensive survey of 13 electrooptic materials regarding the material properties that are pertinent for assessing their use in linear electrooptic modulator applications. The materials covered include ammonium dihydrogen arsenate, ammonium dihydrogen phosphate, barium sodium niobate, bismuth germanium oxide, calcium pyroniobate, copper chloride, lithium niobate, lithium tantalate, potassium dideuterium phosphate, potassium dihydrogen arsenate, potassium dihydrogen phosphate, potassium tantalate niobate, and proustite (Ag_3AsS_3).

A description is given of the principles of electrooptic modulation, emphasizing the importance of crystal symmetry on the electrooptic properties of materials, and including the relationships between the electrooptic, piezooptic, elastooptic, and piezoelectric effects in crystals. Data for each of the 13 materials are presented on crystallographic, optical, electrooptic, photoelastic, piezoelectric, dielectric and thermal properties. Vendor sources are also given.

Linear Electrooptic Modulator Materials, J. T. Milek and S. J. Wells, Electronic Properties Information Center, Hughes, Contract No. F33615-68-C-1225 (January, 1970) (260 pages).

6925 Microwave Acoustics Handbook

This report contains information essential to the design of acoustic filters, signal processors, and other miniature, lightweight devices for use in electromagnetic warfare and in the detection and discrimination of reentry vehicles.

Computations of surface-wave velocity and power-flow angle, and estimates of surface-wave coupling to interdigital transducers are given for various orientations of the following surface-wave substrate materials: $Ba_2NaNb_5O_{15}$, $Bi_{12}GeO_{20}$, CdS, diamond, $Eu_3Fe_5O_{12}$, GaAs, germanium, InAs, InSb, $LiNbO_3$, $LiTaO_3$, MgO, PbS, quartz, rutile, sapphire, silicon, spinel, YAG, YGaG, YIG, and ZnO. Particular cuts of interest are then chosen for more detailed numerical calculations of mechanical and electrical parameters governing acoustic-wave propagation in crystalline media. A list of material constants and a bibliography of 135 surface wave papers are also included.

Microwave Acoustics Handbook: Volume I. Surface Wave Velocities, A. J. Slobodnick, Jr., and E. D. Conway, Air Force Cambridge Research Laboratories, Task No. 5635-03-01, Report No. AFCRL-70-0164 (March, 1970) (354 pages).

6935 Strength of Graphite

A cooperative research effort was undertaken by Avco, Union Carbide, and Southern Research Institute to enhance the understanding of polygraphite as used in typical hardware applications.

A strength analysis was conducted on ATJ-S graphite to relate flaws in a specimen to (1) their ability to act as strength reducers in tension, and (2) to various monitors such as porosity, sonic velocity, and others that relate to the macro- and microstructure. Various methods of nondestructive inspection, such as ultrasonics and radiography, were applied to the billets, blanks, and specimens in an attempt to relate existing inspection techniques to ultimate performance of a specimen. The major strength reducers in ATJ-S were found to be disparate voids, void clusters, and large porous zones. Further, the strength was found to be a smooth function of open porosity ranging from the precursor to the fully densified form. Velocity and electrical resistivity were good monitors of open porosity, but not of disparate flaws. A suitable method of preselecting disparate flaws in all cases was not found. Except for the disparate specimens with unique flaws, this graphite responded in a way suggesting an orderly relation to some parametric analyses, and fracture seemed to be described by uniform distributions. A failure mode and criteria are discussed.

A Strength Analyses of a Polygraphite, C. D. Pears and H. G. Sanders, Southern Research Institute, Contract No. F33615-67-C-1523, Report No. AFML-TR-69-204, Part II (February, 1970) (691 pages, 26 tables, 285 figures).

6936 Transparent Ceramic Armor

General Electric Company's Space Sciences Laboratory has reported on efforts to produce optically transparent magnesium aluminate spinel ($MgAl_2O_4$) intended for use as a replacement for glass in transparent-armor applications.

Spinel ingots were prepared using three fusion processes including (1) crucible melting by induction and radiant heating, (2) resistance heating in graphite containment units, and (3) arc melting using submerged electrodes. The ingots were examined visually and with a light microscope to determine areas of optical transparency.

Arc melting afforded the most rapid melt down and ease of containment, although the lack of controlled solidification and constant melt agitation always resulted in porous ingots of mixed phases.

Ingots produced in the resistance-heating melter contained areas of optically transparent material. The stock material in this case was spinel of near stoichiometric composition which had been previously arc melted. Ingot-solidification rates of 1/2 to 1 mm per minute were required to produce the transparent areas.

Feasibility Study for Producing Transparent Spinel ($MgAl_2O_4$), A. Gatti and M. J. Noone, General Electric Company, Contract No. DAAG46-69-C-0096, Report No. AMMRC CR 70-8 (February, 1970) (29 pages, 5 tables, 15 figures).

6938 Beryllium Oxide

The melting point and phase transition temperature of beryllium oxide has been measured using a thermal-arrest technique developed by General Electric Company personnel. Measurements were made in a tungsten capsule on sulfate-derived BeO that was at least 99.8 percent pure.

The melting point of BeO was determined to be 2430 C with a probable uncertainty of not more than ± 10 C. The α-β transformation was observed at 2095 C (on heating) and 2058 C (on cooling). No claim was made regarding the significance of the transformation temperature in view of the observed hysteresis and a reported dependency on source and purity.

The Melting Point and Phase Transformation of Beryllium Oxide, R. E. Latta, E. C. Duderstudt, and R. E. Fryxell, General Electric Company, Contract No. AT(40-1)-2847, Report No. GEMP-736 (April, 1970) (4 pages, 1 table).

6939 Test Methods for Brittle Materials

Southern Research Institute is conducting a research study directed at obtaining a quantitative evaluation of test methods for brittle materials. This report describes the work completed under the preliminary phase of the program. The brittle material used in the study was a high-purity, aluminum oxide ceramic produced by a commercial supplier. The alumina ceramic was manufactured in 13 different blank shapes, each representing a particular specimen configuration.

An objective of the study was to determine whether a ceramic material produced in a variety of specimen configurations has uniform strength, microstructure, and density. Of the 13 blank types investigated, 10 demonstrated acceptable uniformity and reproducibility, one requires minor modifications, and two require additional work.

The only variables that correlated with strength on first inspection were fired density and a production figure of merit. There was not sufficient data to determine whether a strength-grain size correlation existed. Micro specimen fractology showed that the stronger specimens usually had rough undulating fracture surfaces, while the fracture surfaces of weak specimens were smooth and planar.

A Quantitative Evaluation of Test Methods for Brittle Materials, C. D. Pears, et al, Southern Research Institute, Contract No. AF33(615)-3265, Report No. AFML-TR-69-244, Part I (March, 1970) (228 pages, 10 tables, 132 figures).

6954 Glass for Deep-Submergence Use

This report was prepared by the National Materials Advisory Board to explore and determine the best course of future investigations to obtain the information necessary for the proper use of glass as a structural material, particularly for deep-submergence use.

The first part of the report deals with needed research in the areas of (1) strength of glass and failure mechanisms, (2) glass strengthening techniques, (3) the influence of structure and dynamic processes (e.g., ion migration) on the chemical strengthening process, (4) glass ceramics, including fundamental studies of the crystallization process and products, and (5) fundamental properties of glass (e.g., elastic constants, specific heat).

The second part of the report presents a summary of available scientific knowledge that bears on the recommendations made in the report and is divided into seven parts: strength of glass, chemical strengthening, other methods of strengthening, transport properties in glass, glass structure, vibrational properties of glass, and glass ceramics.

Fundamentals of Massive Glass as a Naval Structural Material, National Materials Advisory Board, Contract No. N00014-67-A-0244-0009 (March, 1970) (98 pages, 5 tables, 8 figures).

6960 Thermal-Shock Resistance of Graphite

A simplified test was developed at Oak Ridge National Laboratory for ranking graphites in terms of their thermal-shock resistance. The test consists of heating thin disks of graphite at the center with an inert-gas shielded-arc nonconsumable-electrode welder. Several disks of each graphite are heated at different but constant power levels. The minimum power input to the welder that will consistently cause the graphite to fracture is determined. The graphite that requires the highest power level to produce a fracture is the one most resistant to thermal shock. Although approximately 30 specimens of each graphite must be tested, the time required for each test is so short that several graphites can be ranked in a short time. The results of thermal rupture tests on 22 different graphites are presented in Figure 6960-I.

The most thermal-shock-resistant graphite tested was ZTA graphite, which was also the most anisotropic material tested. Since the specimens were all oriented so that the plane of the disk corresponded to the plane of isotropy, the ability of ZTA graphite to withstand thermal gradients in the across-grain direction is unknown. AXM and AXF-9Q graphites, which are apparently isotropic, exhibited good thermal-shock resistance. In addition, these two graphites have extremely high coefficients of thermal expansion.

The rankings of 11 grades of graphite determined by figures of merit did not correlate well with their rankings obtained from the task. These results indicate that the figures of merit, $\sigma_f/E\alpha$ and $k\sigma_f/E\alpha$, should not be used in the selection of thermal-stress-resistant graphites. The thermal-shock test is recommended as a tool for screening graphites for applications where the thermal environment is similar to that of the test specimen.

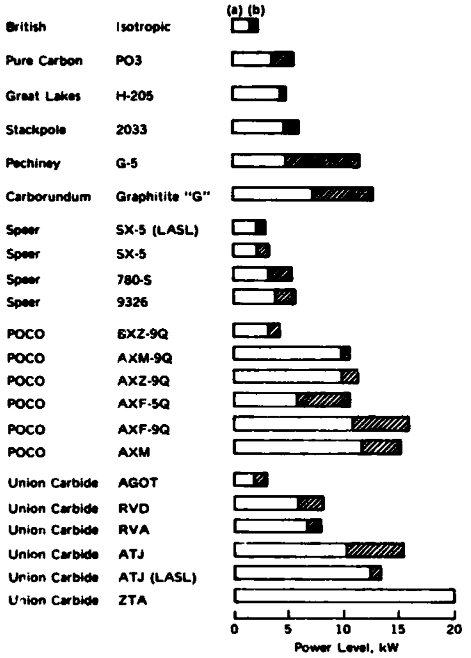

Figure 6960-I. Thermal Rupture Resistance of 2-In.-Diam Graphite Specimens. (a) Lowest Power at Which Fracture Occurred. (b) Highest Power at Which a Specimen Did Not Break.

Determination of Relative Thermal Rupture Resistances of Graphite, G. T. Yahr, Oak Ridge National Laboratory, Contract No. W-7405-eng-26 (January, 1970) (44 pages, 4 tables, 18 figures).

6961 Mechanical Behavior of Graphite

This report from Oak Ridge National Laboratory describes the stress-strain responses of nuclear-grade, or equivalent, graphites under monotonic and cyclic loading conditions. Both stress-versus-longitudinal- and stress-versus-lateral-strain data are considered, and it is shown that consistent patterns of behavior are identifiable from the results. These include differences in deformation resistance in tension and compression, and differences in strain-rate data for the two types of loading.

When a specimen that has been preloaded in compression is cycled in compression between zero and given maximum stress levels, three behavioral patterns are observed. When the maximum stress levels are continually increased and all are greater than the preload value on each subsequent cycle, the hysteresis loops become larger and the paraelastic moduli decrease with increasing maximum stress. Cycling between zero and the preload stress level produces hysteresis loops that do not change with cycle number and the paraelastic moduli remain the same. However, the loops translate along the strain axis for the first few cycles, after which the loops coincide.

Finally, cycling between zero and a fixed maximum value which is less than the preload stress produces hysteresis loops that are essentially invariant both in size and location with cycle number. In a specimen that is loaded, partially unloaded, and reloaded, hysteresis loops are formed by the stress-versus-longitudinal-strain and stress-versus-lateral-strain curves. Also, the reloading curves approach what would have been extensions to the initial loading curves more rapidly than for the case of full unloading. The approach to the extension of a continued loading curve on reloading is often assumed. Here, this postulate is shown to be supported by data obtained from tests designed to examine its validity.

The use of heat treatment in the graphitization temperature essentially removes the effects of prior deformation, so far as stress-strain response is concerned. However, these heat treatments were more successful in removing the prior-deformation histories of ATJ and RVD graphites than of EGCR-type AGOT graphite. Careful use of this technique is shown to be of unique benefit for making comparisons of the stress-strain behaviors of a single graphite specimen under different loading histories.

The Mechanical Behavior of Artificial Graphites as Portrayed by Uniaxial Tests, W. L. Greenstreet, et al, Oak Ridge National Laboratory, Contract No. W-7405-eng-26 (December, 1969) (213 pages, 1 table, 27 figures).

6962 Optical Materials

This EPIC document was prepared to provide infrared refractive-index information on optical materials with emphasis on high-temperature utilization. Refractive-index data and extinction coefficients are provided for the infrared region for silicon, germanium, zinc sulfide, cadmium telluride, zinc selenide, silica, calcium fluoride, magnesium fluoride, aluminum oxide, magnesium oxide, aluminum, gold, and silver. Data showing the dependence of these optical constants on wave length, temperature, crystal form, film-preparation technique, and radiation are presented.

The data sheets are organized in eight chapters comprising a technical introduction, definitions, experimental measurement techniques, problems associated with films, and refractive-index data for semiconductors, fluorides and ceramics, and metals.

Refractive Index of Optical Materials in the Infrared Region, A. J. Moses, Electronic Properties Information Center, Hughes, Contract No. F33615-68-C-1225 (January, 1970) (246 pages).

6963 Strength of E-Glass Fibers

A study was made by General Electric of the strength of E-glass fibers as affected by processing factors controlling the homogeneity and microstructure of the glass. Previous work had shown the existence of macro- and microinhomogeneities in E-glass marbles used as feed stock for fiber production. The variables investigated in the present study to learn their influence on fiber strength included (1) pretreatment of the feedstock marbles, e.g., pulverizing, (2) fining temperature, (3) fining time, (4) the use of mechanical mixing during fining, and (5) the fiber-test environment during strength testing.

Considerable difficulties were experienced in achieving a satisfactory degree of glass homogenization. This situation made it practically impossible to define a "typical" microstructure for fiber-drawn E-glass and, therefore, to define changes in the microstructure as affected by the processing variables. Fiber strengths (intrinsic) measured at liquid-nitrogen temperatures, where stress-corrosion phenomenon should be absent, were particularly sensitive to variations in structure of the glass. Stress-corrosion mechanisms significantly influenced the room-temperature strength of the glass so that quality improvements occasionally revealed by intrinsic strength measurements were not reflected in the room-temperature strengths.

Anomalies observed in strength data of glass fibers subjected to similar melt processing and between groups of fibers from the same melt were attributed to the difficulties in obtaining representative random samples from a nonhomogeneous glass batch.

Relationship of Microstructure of Glass Fiber to Strength, D. L. Hollinger and H. T. Plant, General Electric Company, Contract No. N00019-69-C-0138 (March, 1970) (86 pages, 34 tables, 11 figures).

DIBORIDES ARE SUCCESSFULLY EVALUATED AS LIFTING REENTRY VEHICLE COMPONENTS

Diboride composite materials based on zirconium diboride or hafnium diboride have been successfully simulation-tested as hypersonic leading edges. A previously proven experimental test procedure at Bell Aerosystems, which simulates the thermal-stress environments that a hypersonic leading edge would experience during a flight trajectory, demonstrated the excellent potential of these diboride materials for lifting (high L/D) reentry vehicle nose caps and leading edges. ManLabs, Inc., under AFML Contract AF 33(615)-3671, has developed, characterized and optimized refractory ceramic materials based on zirconium diboride and hafnium diboride both with and without silicon carbide and/or carbon powder. At Bell Aerosystems, leading-edge specimens composed of ZrB_2, ZrB_2 + SiC, ZrB_2 + SiC + C, and ZrB_2 + C were exposed to sequential maximum heat-flux rates of 75 BTU/ft^2-sec and 125 BTU/ft^2-sec. These heat-flux rates correspond to simulated boost-glide reentry flight trajectories for maximum wing loadings of 20 lb/ft^2 and 100 lb/ft^2, respectively. None of the four materials failed either during or after the two simulated boost and reentry cycles. Results of an earlier study at Bell Aerosystems specified that the simulated 100 lb/ft^2 wing loading in conjunction with a maximum reentry heat flux of 125 BTU/ft^2-sec would simulate the most extreme trajectory expected for hypersonic leading edges. On the basis of the completely successful testing of the four above-mentioned materials, two other leading-edge specimens, ZrB_2 + SiC and HfB_2 + C, were subjected to four cycles of the 100 lb/ft^2 - 125 BTU/ft^2-sec environment and did not fail. This testing sequence corresponds to four 1800-second fast boost and glide reentry flight trajectories. The short trajectory time of 1800 seconds also produces more severe thermal-stress effects than if a longer flight time were programmed.

Under another program with ManLabs, Inc., AFML Contract AF 33(615)-3859, a similar composite, HfB_2 + SiC, was exposed to thirteen cyclic arc-plasma tests, each having an 1800-second duration. Each cycle simulated the environment imposed on a 3-in.-radius nose cap of a vehicle moving at 20,000 to 22,000 ft/sec at an approximate altitude of 200,000 feet. The material exhibited surface temperatures of nominally 5000 F, which closely represents the maximum temperature during the glide portions of reentry trajectories. No recession of the material resulted, and only a small surface layer, less than 0.010 inch deep, evidenced a predicted compositional change.

These results are extremely important for reusable spacecraft, space-transportation systems, hypersonic cruise vehicles, and other high-temperature aerospace applications. The excellent oxidation resistance of the diboride materials makes them the leading candidates for reusable nose caps and leading edges of vehicles designed for either minimum downrange or maximum crossrange considerations, where presently envisaged trajectories could extend between 1800 and 7200 seconds. Further discussion of these tests and material characterizations are given in AFML Technical Reports 68-190 and 69-84 which are listed in this issue of CAB under Accession Nos. 4037 and 4337, respectively.

Prepared by: J. R. Fenter and J. J. Krochmal
Ceramics and Graphite Branch
Metals and Ceramics Division
Air Force Materials Laboratory

DCIC SPECIAL REPORTS

Title	Source of Availability	Report Designation
	1968	
A Review of Glasslike Carbons	DCIC*	DCIC 68-2
	CFSTI** or DDC***	AD 668 465
The Evaluation and Interpretation of Mechanical Properties of Brittle Materials	DCIC	DCIC 68-3
Graphite Composites for Re-Entry Vehicles (a classified report/limited distribution)	DCIC	DCIC 68-4
	1969	
Ceramic Armor Symposium****		
Part I, Proceedings	DCIC	DCIC 69-1, Part I
Part II, Proceedings (classified)	DDC	AD 502 440
Part III, Bibliography	DCIC	DCIC 69-1, Part III
Surface Energies of Ceramic Materials	DCIC	DCIC 69-2
	CFSTI/DDC	AD 691 019
Bibliography on Ceramic Fibers and Composite Materials		
Part I, Literature	DCIC	DCIC 69-4, Part I
	CFSTI/DDC	AD 701 118
Part II, Patents	DCIC	DCIC 69-4, Part II
	CFSTI/DDC	AD 701 119
Summary of Papers, 9th Biennial Conference on Carbon, June 1969	American Carbon Committee 102 Mineral Industries Bldg. The Pennsylvania State University University Park, Pennsylvania 16802 Attn: Dr. P. L. Walker, Jr. (The cost is $8.00)	
Ceramic R&D Programs, Part I, Air Force	DCIC	DCIC 69-5, Part I
	DDC	AD 860 094
Part I, Supplement	DCIC	DCIC 69-5, Part I Supplement
	DDC	AD 867 197
Ceramic R&D Programs, Part II, Army	DCIC	DCIC 69-5, Part II
	DDC	AD 865 348
Ceramic R&D Programs, Part III, Navy	DCIC	DCIC 69-5, Part
	DDC	AD 866 096

*Defense Ceramic Information Center.

**Clearinghouse for Scientific and Technical Information, Springfield, Virginia 22151.

***Defense Documentation Center, Cameron Station, Alexandria, Virginia 22314. (Qualified requestors only)

****Parts I and III are available only from DCIC at a cost of $15 for both parts.